Recognition of Targets by Linear and Non-Linear (Delta K) Processing of Multi Frequency Data

D.T. Gjessing, J. Saebboe, OE. Helleren
Triad AS, Storgata 6, 2000 Lillestroem
Norway

triad@triad.no

ABSTRACT

Multi frequency data from continuous wave radar is used to recognize air, sea and land targets. Target range profile data is extracted both from the linear combination of the frequencies and the non-linear Delta K processing. The results are discussed in light of the motion pattern and the vibration of the target. Continuous wave data offers long integration time for Doppler processing, which can be used to get high-resolution Doppler signatures of the targets. These features are discussed as target classifiers. The paper describes the technology and presents some experimental results. The application and limitations of the technology is discussed with focus on integration in a pulsed system.

1.0 INTRODUCTION

Using a multi frequency continuous wave or range gated radar system we can sample the targets Doppler shifts at several frequencies in parallel.

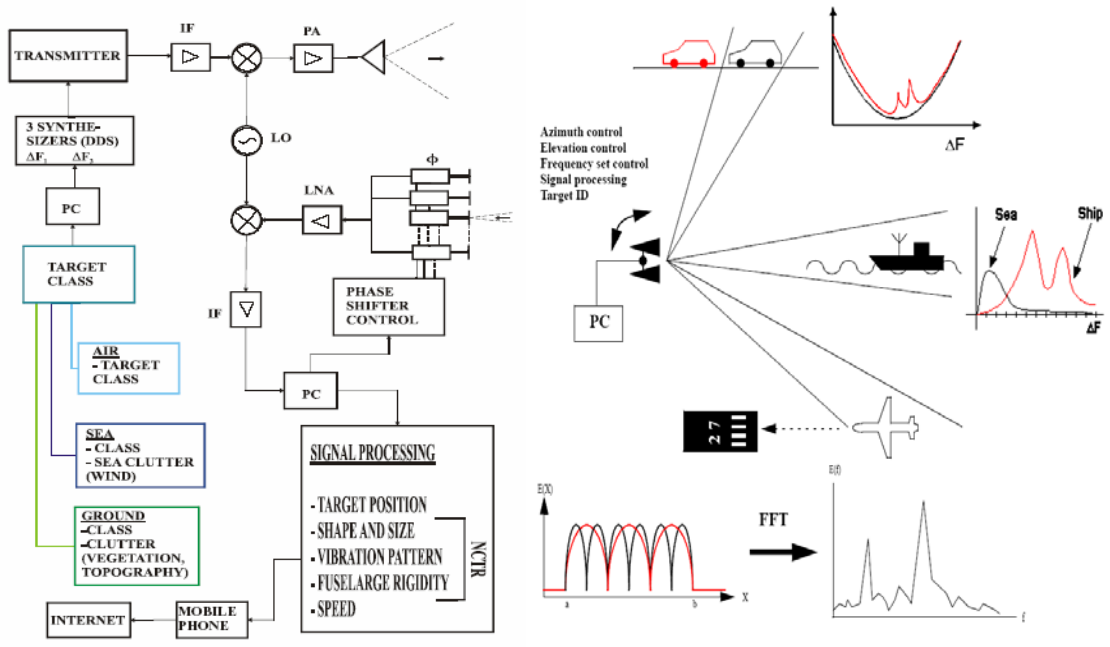

Figure 1: To the left in the figure is an overview of the system under developing. To the right the fundamental idea of operation of the system is presented.

Paper presented at the RTO SET Symposium on "Target Identification and Recognition Using RF Systems", held in Oslo, Norway, 11-13 October 2004, and published in RTO-MP-SET-080.

The multi frequency return can be processed linear or by non-linear ΔK. The author's organisation is developing a range gated radar system for multi frequency experiments for targets at air, sea and land. An overview of this system is given in figure 1. In our stepwise development of this system we execute experiments and simulations as to understand the fundamental theory and the possibilities for our system.

Office of Naval Research (ONR) is sponsoring parts of the work presented in this paper.

2.0 BASIC THEORY

2.1 Electromagnetic theory

When solving the basic scattering equations the following very simple relationship results after several approximations:

$$E(K) \sim \int \sigma(r) e^{-jK \cdot r} dr$$

Here $\mathbf{r}$ is the position vector, $\mathbf{K}$ the scattering wave number, σ the scattering cross section on voltage basis.

If the scatterers are distributed in space along the direction as a delay function $\sigma(\mathbf{r})$, the field strength as a function of wave number of the backscattered wave is the Fourier transform of this delay function. Hence, if we measure $E(K)$ (the received fields as function of wave number), we can find the spatial distribution of the target by an inverse Fourier transformation process:

$$\sigma(r) \sim \int E(K) e^{jK \cdot r} dK$$

The target can also be described in the $\Delta\mathbf{K}$ domain using an autocorrelation function

$$R(\Delta K) \sim e^{-j(\Delta K)z} \int R_{\sigma}(r) e^{jKr} e^{j(\Delta K)r} dr$$

Here z is the distance to the target. Different type of targets will have different autocorrelation function as seen in figure 2.

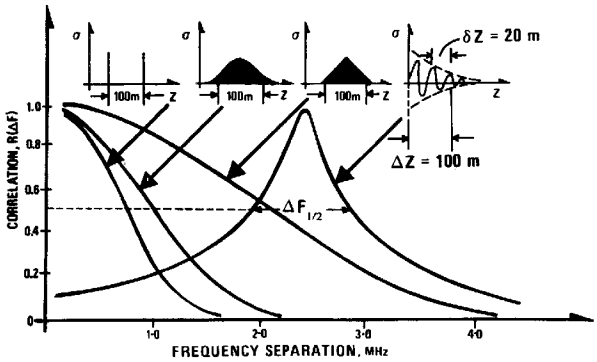

Figure 2: Different type of targets has different correlation functions.

2.2 DK processing

Linear processing of multi frequency data combines the different frequency components that are obtained in parallel or stepwise and gives range resolution through a Fourier transform of this.

In ΔK processing each frequency component is selected through narrowband filters. These frequency components are then multiplied with each other to form a set of ΔK timeseries. Using unequal spacing between the frequencies it is possible to obtain a higher number of unique frequency spacing than the number of frequencies used. For valid Coulomb rulers we obtain $N = \left[n(n-1)\right]/2$ frequency spacing by using *n* frequencies.

As a basic example of the ΔK processing we use a target that consist of two corner reflectors of unit amplitude spaced *z* meters apart in radial distance. The target moves at a given speed in outward radial distance. A timeseries for a single frequency component is given by

$$V_i = \exp\left(jK_i r_0\right) + \exp\left(jK_i r_1\right).$$

Here K_i is the scattering wave number for frequency component *i*. r_0 and r_1 the radial distance to the two scattereres, which is a function of time when the target moves.

A ΔK time series is found by multiplying two frequency components as

$$V_k conj(V_l) = \exp(j\Delta K r)\left[1 + \exp(-jK\Delta r) + \exp(jK\Delta r)\exp(j\Delta K\Delta r) + \exp(j\Delta K\Delta r)\right].$$

Here *K* is the scattering wave number of the carrier, Δr the distance between the scattering elements, *r* the distance to the first scattering element and ΔK the difference wave number.

We see that the first term in the above equation, $\exp(j\Delta K r)$, is recognized as the ΔK channel Doppler shift. This can be removed by mixing. The second term, $\exp(jK\Delta r)$, is dependant on the 'carrier frequency' and Δr. Since Δr is supposed be to unknown, we cannot predict this term. If Δr is vibrating sufficiently with time/range it is averaged to zero. The desired signature $\exp(j\Delta K\Delta r)$ lies in term 3 and 4. If the term $\exp(jK\Delta r)$ is not averaged the overall result is a signature that is a summation of the desired signature and a phase shifted version of it. Note that for non-vibrating objects it is possible to modulate the transmitted signal with a random phase shift or a frequency sweep to average out the unwanted interferences.

A simple simulation illustrates the dependence on the targets motion pattern. Our target consists of two identical reflectors spaced 10 meters apart in radial direction. The simulated carrier frequency is 3.4 GHz. The simulated target is at 8000 m range and moving 100 meter in one second. The separation between the scatterers is varying randomly within 4 centimeters in radial direction during motion. In figure 3 results form the simulation is presented in 9 subfigures. The subfigures are numbered from 1 in the upper left to 9 in the lower right. 1-6 are intensity plots with the y-axis as range/time and the x-axis as ΔF 0-25 MHz (left to right). The contents of the subfigures are:

1. Term 1, $\exp(j\Delta K r)$, from the ΔK function. This is the ΔK Doppler signal. We clearly se that as the target moves the Doppler signal from the higher ΔK channels is of higher frequency.

2. Term 2, $\exp(jK\Delta r)$, from the ΔK function. As this term is dependant on the carrier wave number K and not the separation ΔK, there is no variation along the frequency axis. The randomness of the target element vibration, Δr, is seen along the y-axis.

3. Term 3, $\exp(j\Delta K\Delta r)\exp(jK\Delta r)$, from the ΔK function. We can se that the wanted signature is randomly shifted along the frequency axis.

4. Term 4, $\exp(j\Delta K\Delta r)$, from the ΔK function. This is the desired signature of the target.

5. The whole ΔK function. Through its randomness it is possible to view the contours of the ΔK signature.

6. The direct multi frequency function. Here the x-axis is frequency from carrier (left) up to carrier + 25 MHz (right). No particular signature is visible.

7. A time sample of one of the received channels.

8. The average in time/range of the signals the DK function (sub image 5, solid line) and the multi frequency function (sub image 6, dashed line). We can see that there is more coherent contribution to the signature when averaging over ΔK than over plain multi frequency.

9. The averages in sub image 8 have been normalized. The solid line is the desired signature of the target. The dashed line is the simulated ΔK signature and the dotted line is the multi frequency signature. We can se that the simulated ΔK signature nearly overlaps the expected signature whereas the plain multi frequency signature contains errors.

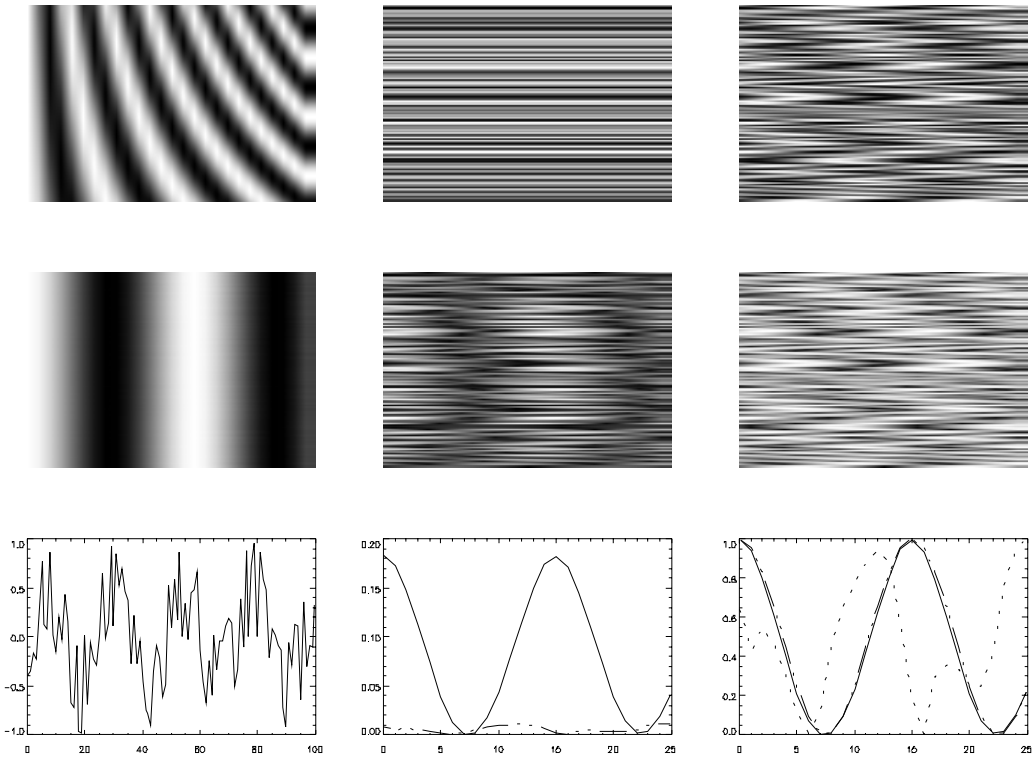

Figure 3: The subfigures are numbered [1,2,3] from left to right in the upper row, [4,5,6] in the middle row and [7,8,9] in the lower row. Each subfigure is commented in the text.

2.3 Delta K estimation error function

Setting the starting range to zero we can simplify the a single DK channel response to

$$V_k conj(V_l) = 2\exp(j(k_k - k_l)\Delta r)\left[\cos(j(k_k - k_l)\Delta r) + \cos(j(k_k + k_l)\Delta r)\right].$$

Here the target consists of two corner reflectors one placed at zero meters and one placed Δr in radial direction. k_k and k_l are the wave numbers of which the difference wave number in this example arises from. Investigating this equation we see that the first cosinus term represent the desired difference wave number amplitude, while the second term represents the rapidly fluctuating estimate error. We see that the latter expression depends on the sum of the wave numbers and the distance between the scattering elements.

In figure 4 this latter function is evaluated for two different carrier frequencies, increasing separation between the scattering elements and a carrier sweep.

Evaluating the subfigures in figure 4 we find

1. Error function evaluated for a carrier frequency of 5 GHz. As the distance between the scattering elements increases the error function rotates at a constant ratio defined by the sum of the wave numbers. As we sweep the carrier towards higher frequency, thus increasing the sum of the wave numbers the rotation ratio as a function of target element separation increases.

2. The same as subfigure 1 with 10 GHz carrier. We can se that the ratio of rotation as a function of range between the scattering elements has increased. This means that a vibration of less displacement than can average out the estimation error for using higher carriers.

3. We can se that using a carrier sweep to average out the estimation error the sweep length necessary depends on the distance between the target elements and not the carrier frequency.

4. The same as 3.

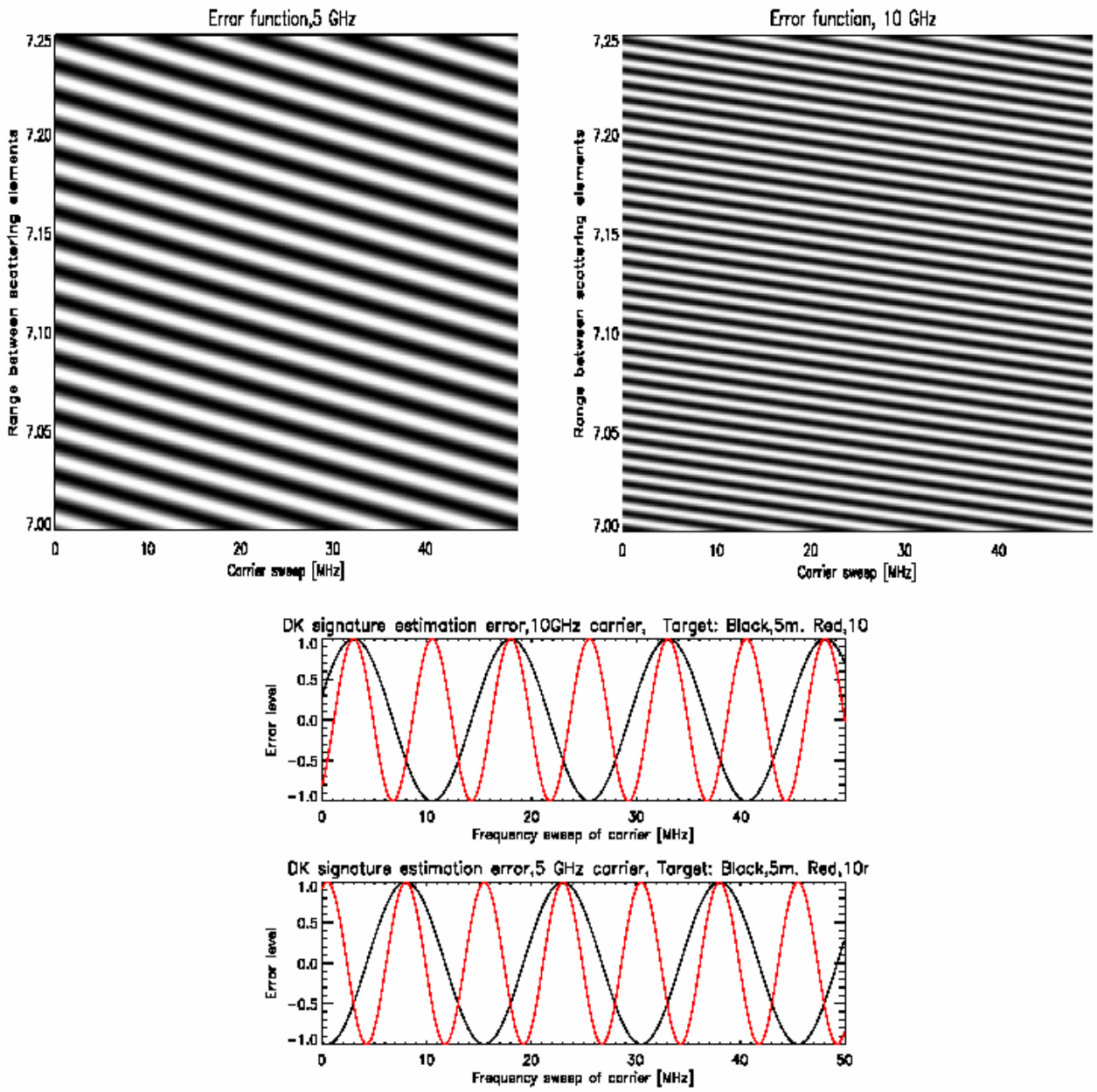

Figure 4: The subfigures 1 upper left 2 upper right, 3 middle and 4 lower are commented in the text.

3.0 CLUTTER VIEWED IN THE FREQUENCY DOMAIN

3.1 Sea surface clutter

The dominating sea surface gravity capillary wave is described by the basic wave equation

$$\omega = \sqrt{gK}$$

The phase velocity of this wave is then given by

$$v = \frac{\omega}{K} = \sqrt{\frac{g}{K}}$$

The dispersivity of this equation is seen in figure 5.

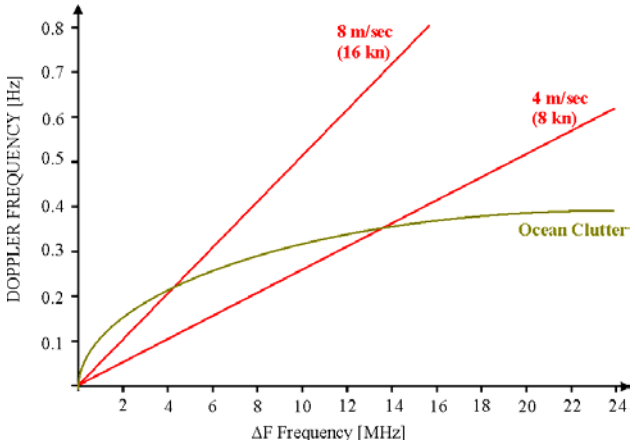

Figure 5: The dispersivity of the sea surface waves gives rise to a characteristic Doppler signature in the frequency domain.

Using the wind as the driving force this velocity cannot exceed that of the wind. Setting the phase velocity of the wave equal to the wind speed we can construct the minimum coupling wave number as

$$K_{\min} = \frac{g}{V_{vind}^2}$$

If EM waves have the same wave number they will couple to these ocean waves.

$$K_{EM} = K_{Ocean} = \frac{4\pi \sin(\theta/2)}{\lambda} = \frac{4\pi F \sin(\theta/2)}{c}$$

This equation leads us to a frequency (or difference frequency) that for maximum coupling to the wind driven waves as

$$F = \frac{cg}{4\pi V^2 \sin(\theta/2)}.$$

For backscattering the sinusoidal term equals unity. The same expression is valid for matching the ocean waves by ΔF by substituting F with ΔF in the equation.

Defining a 10dB width of this spectrum we can form a function that tells where the interaction between the EM waves and the sea surface waves is dominating. Avoiding these regions, as seen in figure 6, is essential for suppression of the sea surface clutter.

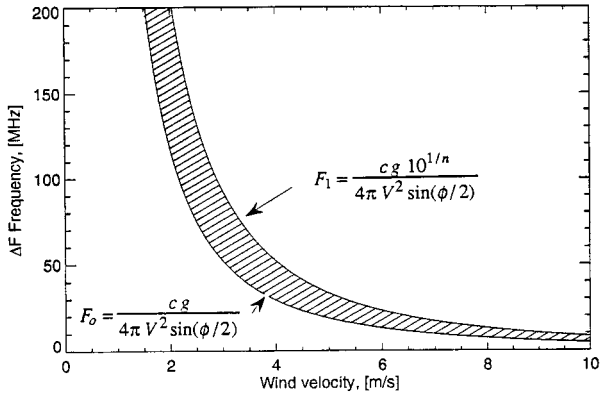

Figure 6 : Region of Interaction between EM waves and sea surface waves

3.2 LAND clutter

For many stochastic processes is popular to use the Komolgorov spectral function. Kolomgorov characterize randomly orientated scatterers in wave number space as $\Phi(K,\omega) = K^{-n}$ where n in most cases is -11/3. Applying this theory to a forest background we can use the dominating distance between the trees as the dominant scale. This is illustrated in figure 7, left. Dealing now with targets of rectangular shape that corresponds to a ΔK frequency signature of the form $\sin(x)/x$. This gives a signal to clutter structure as illustrated in the figure 7, right.

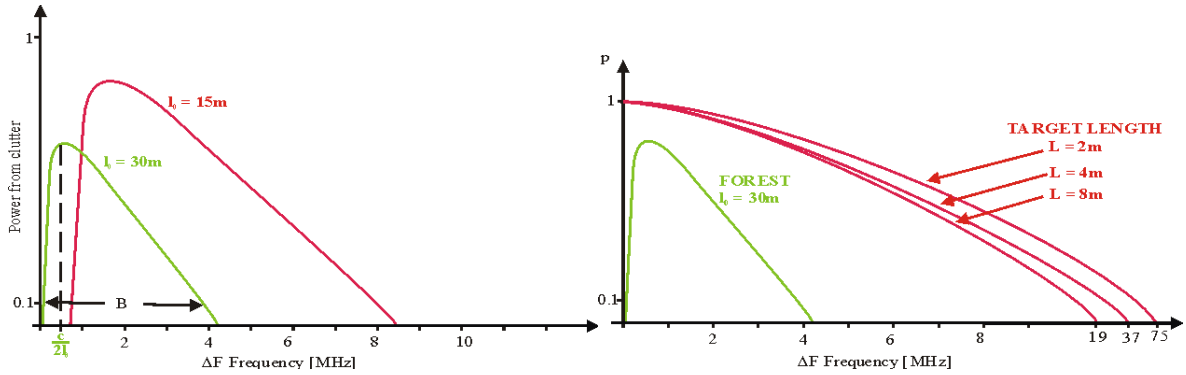

Figure 7: Left, two forests with different dominating spacing between the trees have different ΔK frequency signature. Right, a typical target of less length than the dominating clutter scale will have a larger bandwidth in the ΔK frequency domain.

4.0 EXPERIMENTAL VERIFICATION

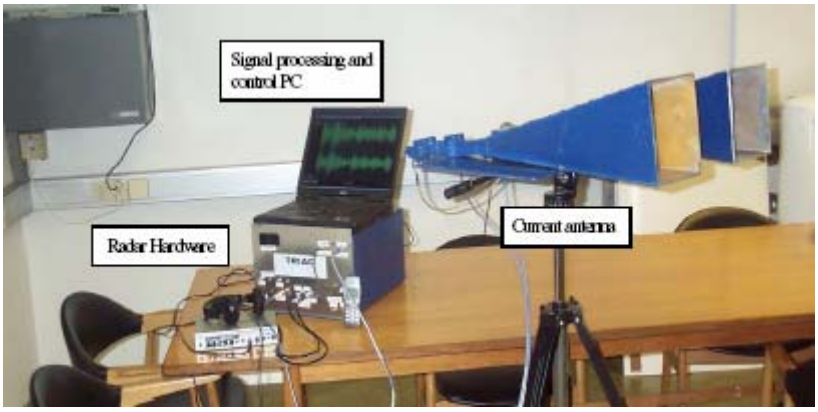

Figure 8: Experimental hardware.

Our experimental radar, which performs a subset of the system presented in figure 1, is seen in figure 8 and can be summarized by the following statements:

- Size of radar 20x30x40 cm
- Size of antennas 20x20cm aperture, 60 cm length
- Weight of radar with antennas appx 12 kilo
- Detection range for a target of $\sigma = 20m^2$ is 80 km
- Receiver noise factor 1 dB
- Transmitted power up to 10W cw

This experimental radar system was used in the experiments presented in the following subchapters.

4.1 Small boat

A boat with a length 5 meters was the target for a measurement campaign in the Oslo Fjord in Norway. One small corner reflector was mounted in the front of the boat and one in the stern. To frequencies were on the air simultaneously giving data to form one ΔK channel. The measurements were done in backscatter mode with the boat travelling in radial inwards direction. The experiment was repeated several times with different frequency settings to construct a ΔK signature.

The ΔK frequency signature of the target and the ΔK Doppler signature of the target can be seen in figure 9. We can see that the measured points fit well with the theoretical curves.

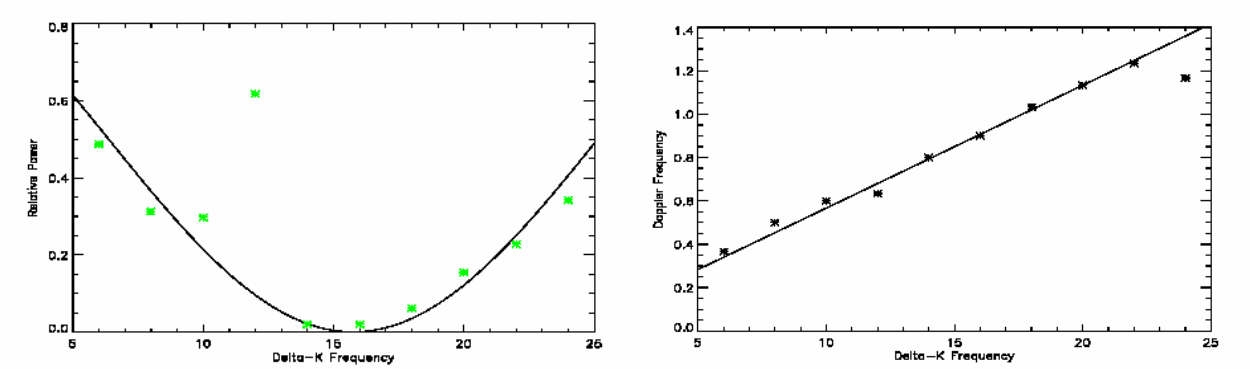

Figure 9: Left: Measured points of the ΔK signature of the target upon the theoretical curve for 5 m spacing. Right: Measured points of ΔK Doppler signature of the target upon the theoretical curve based on GPS measured speed

4.2 Detection and ID of land targets

4.2.1 Calibration

This experiment was conducted by the shore side of the lake Mjøsa in Norway. Two targets of corner reflectors with different spacing were towed on a rope in near radial direction. Transmitting 4 frequencies in parallel we towed each target several times with different frequency sets. Figure 10 presents the measured points from two runs for each target. We can see that the measured points fit well with the theoretical curve.

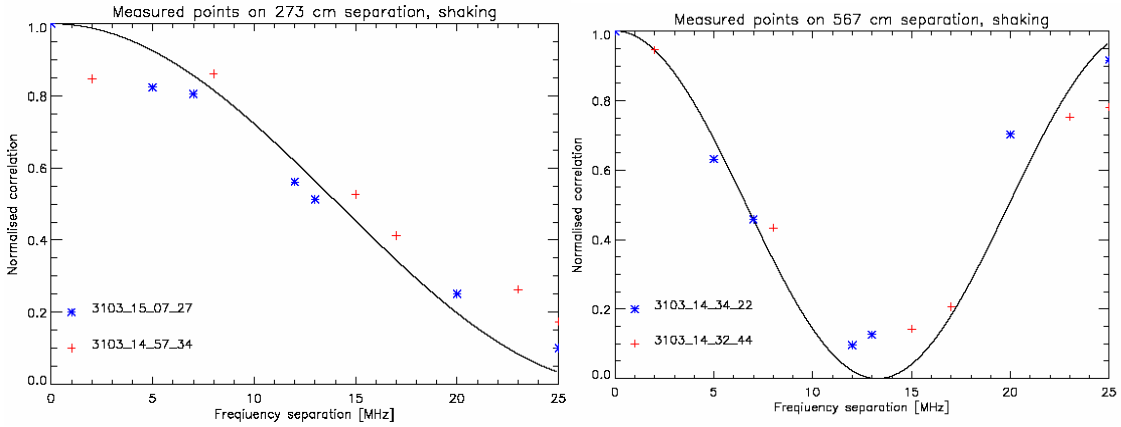

Figure 10: To the left is the signature of a target consisting of two reflectors spaced 275 cm in radial direction. To the right the spacing is 565 cm. Both targets were towed in near radial direction. The reflectors was vibration during motion

4.2.2 Cars with a forest background

This experiment took place at a road with a forest background. The distance to the target was 500 meters. Two cars of same length but of different shape were driving in near radial direction. In figure 11 we can se the difference in their signature.

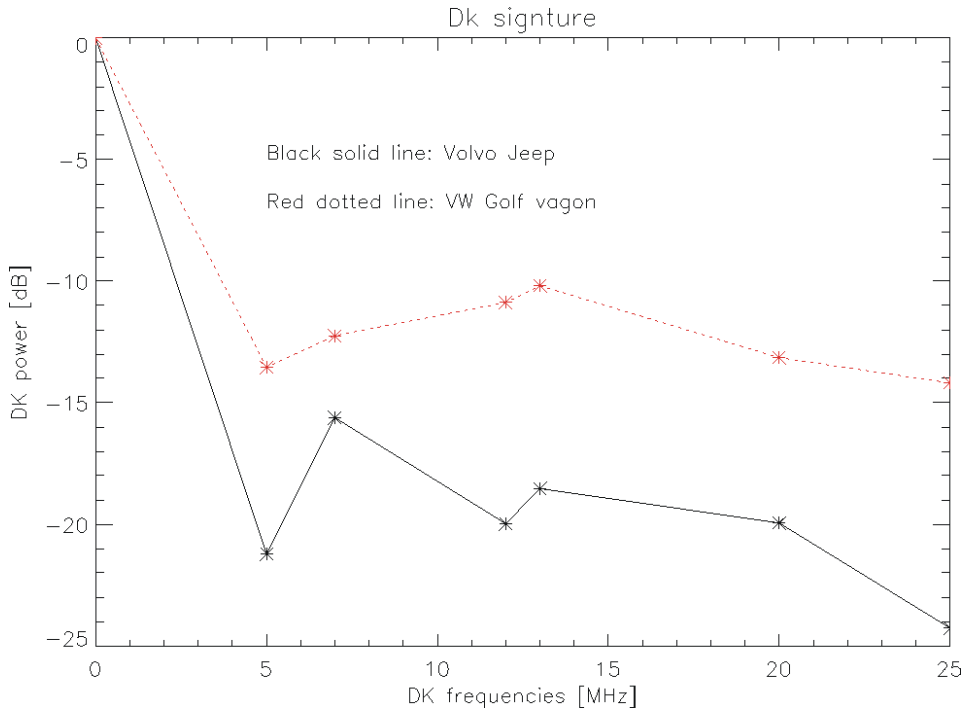

Figure 11: Measured signatures of a military jeep and a VW golf wagon.

4.2.3 ISAR

At the same site as for the calibration experiment two targets of corner reflectors where used in ISAR measurements. A single continuous wave frequency illuminated the corner reflectors that were sliding along a fixed rope.

We present here measurements of a two elements target. The first with a length of 565 cm and the second with a length of 275 cm. The measurements were done in backscatter mode with an aspect angle of 45 degrees. The different targets moved with the same speed and along the same path. Figure 12 displays the smoothed time series for a single channel for the 275 cm target and the same for the 565 cm target.

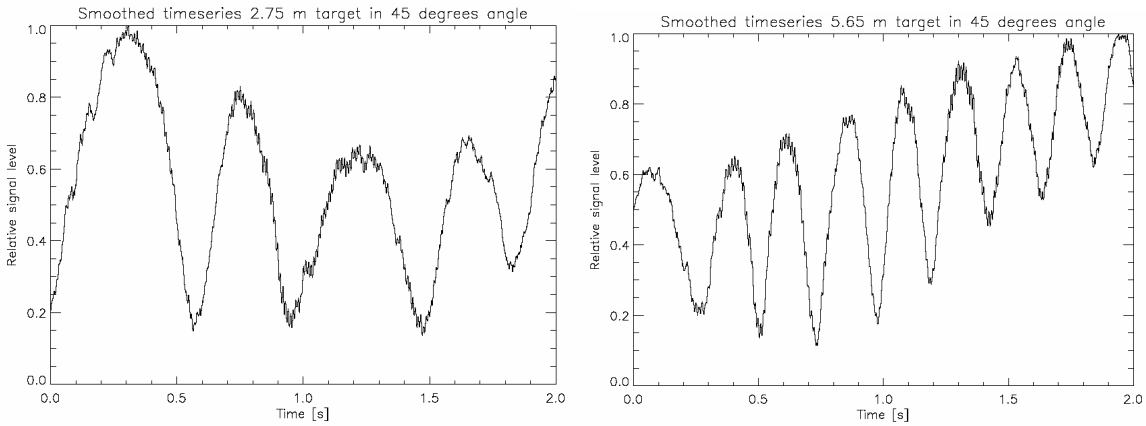

Figure 12: Smoothed time series of a cross range moving target of two corner reflectors spaced 2.75 m Left and spaced 5.65 m right

In figure 12 we can see that the different target lengths modulate the received signal with a different 'frequency'. Using a FFT we can find the frequency. This is presented in figure 13.

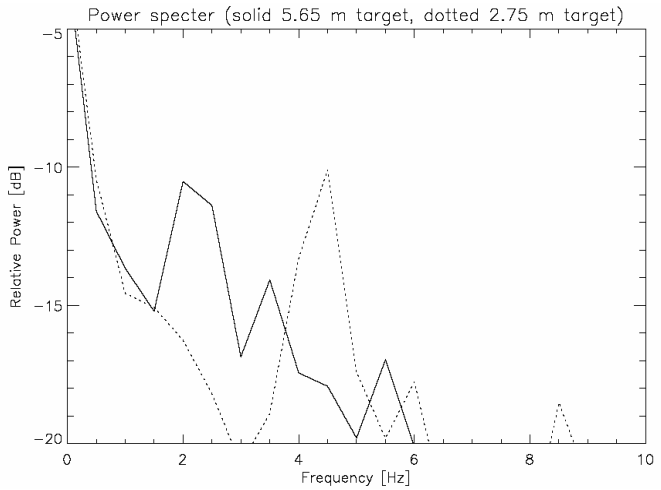

Figure 13: FFT of the ISAR time series. The solid line represents the target of 275 cm. The dotted line represents the 575 cm target. We see that as expected the dominating frequency of the 575 cm target is close to double that of the 275 cm target.

5.0 CONCLUSION

We have presented the fundamental theory around our experimental multi frequency system. From simulations we find the dependency on the target motion pattern to obtain valid results. The simple experiments presented reflect the theoretical values and is a good basis for more advanced measurements.

6.0 BIBLIOGRAPHY

[1] GJESSING, D.T.: 'Remote surveillance by Electromagnetic Waves for Air-Water-Land' (Ann Arbor: Science Publishers, 1978)

[2] GJESSING, D.T.: 'Adaptive Radar in remote Sensing' (Ann Arbor: Science Publishers, 1981)

[3] GJESSING, D.T.: 'Target adaptive matched illumination, principles and applications' (Peter Peregrinus IEE, 1986)

[4] HAYKIN, S.: 'Communication Systems' (WILEY, New York, 1983)

[5] ISHIMARU, A.: 'Electromagnetic Wave Propagation, Radiation, and Scattering' (PRENTICE HALL, New Jersey, 1991)

[6] ISHIMARU, A.: 'Wave Propagation and Scattering in Random Media, volume 2' (ACADEMIC PRESS, New york, 1978)

[7] STRATTON, J.A.:, 'ELECTROMAGNETIC THEORY' (McGraw-Hill, New York, 1941)